Patron: Her Majesty The Queen

ROTHAMSTED RESEARCH

Rothamsted Research
Harpenden, Herts, AL5 2JQ

Telephone: +44 (0)1582 763133
Web: http://www.rothamsted.ac.uk/

Rothamsted Repository Download

A - Papers appearing in refereed journals

Golosov, V., Collins, A. L., Tang, Q., Zhang, X., Zhou, P., He, X. and Wen, A. 2017. Sediment transfer at different spatial and temporal scales in the Sichuan Hilly Basin, China: Synthesizing data from multiple approaches and preliminary interpretation in the context of climatic and anthropogenic drivers. *Science of the Total Environment.* 598 (15 November), pp. 319-329.

The publisher's version can be accessed at:

- https://dx.doi.org/10.1016/j.scitotenv.2017.04.133

The output can be accessed at: https://repository.rothamsted.ac.uk/item/8v463.

© 2017. This manuscript version is made available under the CC-BY-NC-ND 4.0 license
http://creativecommons.org/licenses/by-nc-nd/4.0/

27/03/2019 16:48 repository.rothamsted.ac.uk library@rothamsted.ac.uk

Rothamsted Research is a Company Limited by Guarantee
Registered Office: as above. Registered in England No. 2393175.
Registered Charity No. 802038. VAT No. 197 4201 51.
Founded in 1843 by John Bennet Lawes.

Science of the Total Environment 598 (2017) 319–329

Contents lists available at ScienceDirect

Science of the Total Environment

journal homepage: www.elsevier.com/locate/scitotenv

Sediment transfer at different spatial and temporal scales in the Sichuan Hilly Basin, China: Synthesizing data from multiple approaches and preliminary interpretation in the context of climatic and anthropogenic drivers

Valentin Golosov [a,b,c], Adrian L. Collins [d,a], Qiang Tang [a,d,*], Xinbao Zhang [a], Ping Zhou [a], Xiubin He [a], Anbang Wen [a]

[a] Key Laboratory of Mountain Surface Processes and Ecological Regulation, Institute of Mountain Hazards and Environment, Chinese Academy of Sciences, Chengdu 610041, China
[b] Kazan (Volga region) State University, Kazan 420008, Russia
[c] Faculty of Geography, Moscow State University, Moscow 119991, Russia
[d] Sustainable Agriculture Sciences Department, Rothamsted Research, North Wyke, Okehampton, Devon EX20 2SB, UK

HIGHLIGHTS

- Sediment transfer at multiple spatio-temporal scales was synthesized using different data sources.
- High slope-channel sediment conveyance ratios were observed.
- Both natural and human forces have driven decreases in sediment yield.

GRAPHICAL ABSTRACT

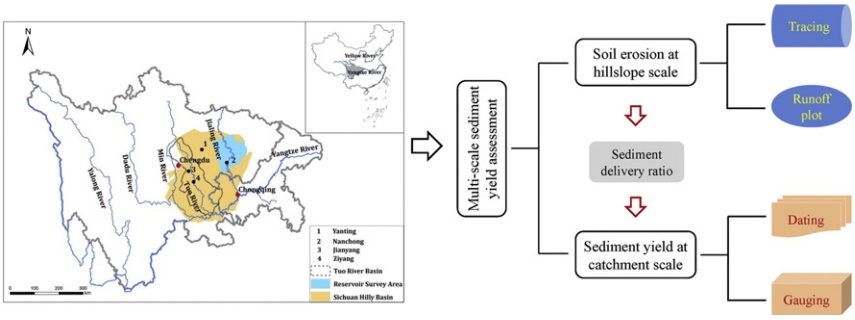

ARTICLE INFO

Article history:
Received 7 February 2017
Received in revised form 18 April 2017
Accepted 18 April 2017
Available online 24 April 2017

Editor: F.M. Tack

Keywords:
Caesium-137 tracing
Sediment delivery ratio
Sediment budget
Sediment transfer
Slope-channel connectivity

ABSTRACT

Quantifying sediment production and transfer at different spatial and temporal scales in a changing environment is critical in understanding the potential effects of climatic and anthropogenic drivers. Accordingly, estimates of soil erosion and sediment production at hillslope field, first-order small catchment (<0.25 km^2) and river basin scales in the Sichuan Hilly Basin of Southwestern China, generated using a variety of techniques, including fallout radionuclide tracing, runoff plot observations, core chronology dating and conventional sediment flux monitoring, were synthesized and interpreted in the context of potential climatic and human controls. Mean annual soil erosion rates ranged from 800 $Mg \cdot km^{-2} \cdot yr^{-1}$ to 4500 $Mg \cdot km^{-2} \cdot yr^{-1}$ on the basis of fallout radionuclide tracing and from 600 $Mg \cdot km^{-2} \cdot yr^{-1}$ to 3300 $Mg \cdot km^{-2} \cdot yr^{-1}$ using runoff plot monitoring on selected cultivated hillslopes. A high slope-channel sediment delivery ratio was observed, meaning that a substantial proportion of eroded sediment was delivered into downstream drainage channels. An obvious temporal trend of decreasing sediment transfer to the river channels in the first-order catchments was identified, which may be driven by change in regional precipitation regime and the implementation of multiple soil conservation and reforestation practices over recent decades.

© 2017 The Authors. Published by Elsevier B.V. This is an open access article under the CC BY-NC-ND license (http://creativecommons.org/licenses/by-nc-nd/4.0/).

* Corresponding author at: Institute of Mountain Hazards and Environment, Chinese Academy of Sciences, No. 9, Block 4, South Renmin Road, Chengdu 610041, China.
E-mail address: qiangtang@imde.ac.cn (Q. Tang).

http://dx.doi.org/10.1016/j.scitotenv.2017.04.133
0048-9697/© 2017 The Authors. Published by Elsevier B.V. This is an open access article under the CC BY-NC-ND license (http://creativecommons.org/licenses/by-nc-nd/4.0/).

1. Introduction

Suspended sediment transport through river channels constitutes a major pathway for the continent-ocean delivery of terrestrial materials (Walling and Fang, 2003; Walling, 2006). It causes many off-site detrimental environmental consequences such as water quality deterioration, channel sedimentation, extreme flooding, and reservoir siltation (Walling and Collins, 2008). Sediment yields at a catchment outlet represent an integrated product of the upstream hydrological processes driving soil erosion and sediment transport, which, in turn, demonstrate high spatial and temporal variability in accordance with regional geographical settings and human disturbances. Specifically, the sediment delivery ratio (SDR) coefficient exhibits a wide range across many landscapes, depending on slope-channel connectivity, the grain-size composition of eroded sediment, and the number and location of buffers and sinks along the hydrological pathways from upland hillslopes to river channels (Walling, 1983; Ferro and Minacapilli, 1995; Walling and Collins, 2008). The SDR also exhibits temporal variations in response to changes in climatic patterns and land use (Van Oost et al., 2000; Wang et al., 2010; Chaplot and Poesen, 2012). It can, however, be difficult to evaluate the specific ways in which different controlling factors contribute to the observed changes in integrated sediment signals in river systems. This challenge is complicated especially in heavily cultivated agricultural regions where population density is high and human disturbances are intensive and interactive (Owens, 2005). Sediment budgeting provides a valuable integration framework for understanding the individual processes of sediment supply, mobilization, transport and storage (Walling, 1983; Walling and Collins, 2008) as well as the ways in which sediment dynamics respond to environmental and anthropogenic controls (Evans et al., 2000). Knowledge of sediment dynamics in a changing environment is required for evaluating the effectiveness of soil conservation practices and designing effective sediment management strategies.

Different levels of resource can be directed towards quantifying the sediment delivery ratio (Owens et al., 1999; Walling et al., 2002), sediment storage in depressions (Walling et al., 2006), and sediment delivery processes linking hillslopes and drainage channels (Oygarden, 2003). Fallout radionuclides have been widely applied as sediment tracers for evaluating soil redistribution rates (Wallbrink and Murray, 1996; Owens et al., 1997; Walling and He, 1997, 1999; Belyaev et al., 2009; Porto et al., 2011; Gaspar et al., 2013; Golosov et al., 2013; Porto et al., 2014) as well as sedimentation rates (Ritchie et al., 2004; Hobo et al., 2010; Hughes et al., 2010). It is essential to place such predictions into the context of soil erosion and sediment transfer rates provided by alternative more traditional procedures and to evaluate the tracing estimates in the context of the sediment budget and the corresponding implications for the magnitude of unmeasured budget components required for budget balance (Collins and Walling, 2004). As reported by Trimble (2009) in the Coon Creek Basin, USA, the catchment sediment budget can be transformed substantially by climatic and anthropogenic changes over relatively short time intervals.

The Sichuan Hilly Basin (SHB) is an undeveloped agricultural region with dense population, which produces a substantial proportion of the suspended sediment loads delivered to the Yangtze River (Lu and Higgitt, 1999; Lu et al., 2003). A variety of human activities over the past few decades have resulted in profound impacts on regional soil erosion and sediment redistribution. On the one hand, soil erosion has been accelerated by intensive land disturbance such as land reclamation, forest destruction and tillage translocation while, on the other hand, noticeable land use change has taken place in conjunction with farmland abandonment and reforestation campaigns. Climate change has also been detected (Zhang et al., 2008), which has triggered substantial changes in sediment redistribution at catchment scale. Against this background, this study aimed to assemble various data sources to evaluate sediment production and transfer at different spatial and temporal scales and to postulate on predominant controls operating on slope-channel sediment delivery in the SHB. Accordingly, data on upland soil erosion, slope-channel connectivity in first-order catchments and downstream suspended sediment yields generated by a range of methods were assembled and integrated. These datasets were taken to represent the fundamental components of the sediment delivery cascade from eroding uplands to downstream monitoring stations.

2. Materials and methods

2.1. Site description

The SHB represents a major agricultural region in China with dense human occupation and suffers from intensive human disturbance by traditional manual farming cultivation. As a result, the magnitude of soil erosion is high and the region serves as a principal source area for sediment delivered to the Yangtze River (Fig. 1). The land use is closely linked to local topography. The SHB is typically fragmented by numerous small first-order catchments comprised of steep concave slopes with gradients deceasing from 20°–25° in the upland areas to 5°–10° in the lowland areas. Large-scale catchments are characterized by wide flat valleys. Surface land is covered by the purple soils, which is classified as an Entisol by the soil taxonomy of the USDA (He et al., 2007). Farmland (upland terraces and orchards) typically accounts for 20–60% of land cover. Crop rotation including corn, sweet potato, rape and wheat has been practiced since the 1980s. The remaining proportions (>25°) of the study areas are woodlands or steep wastelands. The valley bottoms are commonly used as paddy fields. Small reservoirs and ponds are constructed on the lower reaches at the outlets for irrigation purposes, while large dams have been constructed on the main and tributary channels for multiple purposes including hydropower production, flood control and water supply.

Spatially distributed sites were selected to quantify data at different scales using multiple approaches. Four primary study sites (see background data in Table 1) were selected to evaluate mean annual net soil loss from upland cultivated hillslopes (Fig. 1). These sites were selected as being representative of typical agricultural areas in the SHB with soil erosion problems due to farming and associated tillage translocation. Three small first-order catchments were selected to evaluate the mean annual specific suspended sediment yields. The Wujia and Jiliu catchments, in Yanting County, have respective drainage areas of 0.22 and 0.09 km^2. They have similar physico-geographical and land use characteristics, with elevations varying from 420 to 560 m. Catchment surface soils are underlain by horizontally bedded mudstones, siltstones and sandstones from the Jurassic Penglaizhen Group. Local landforms typically comprise steep sandstone cliffs with slopes of 25–30° separated by gentle mudstone and siltstone terraces of <10°. Annual rainfall is 826 mm. The gentle terraces and steep slopes account for one and two thirds of the catchment areas, respectively. The gentle terraces have been cultivated, whereas the steep slopes were originally covered by wild grasses, but have gradually been afforested with cypress trees since the 1970s. The Tianmawan watershed, in Nanchong, has a drainage area of 0.19 km^2 and elevations ranging from 310 to 420 m. It is underlain by horizontally bedded mudstones and siltstones from the Jurassic Suining Group (Zhang et al., 2006a). Local topography typically comprises dozens of small steep cliffs separated by short gentle terraces. The steep cliffs have typical heights of a few meters and are covered by wild grasses and scattered young cypress trees. The gentle terraces with slopes of <10° and lengths of 10–30 m are mostly rain-fed areas. Annual precipitation is ~1010 mm, approximately 70% of which occurs during the wet season from June to September.

Purple soils dominate in all three catchments, but important differences in erosion resistance depend on soil parent material. Due to different proportions of sandstone, the purple soils of the Penglaizhen and Suining Group have relatively high and low erosion resistances, respectively. The cropland ratio in the Tianmawan catchment is 0.45, while that for the other two catchments is 0.25. Each of the study catchments

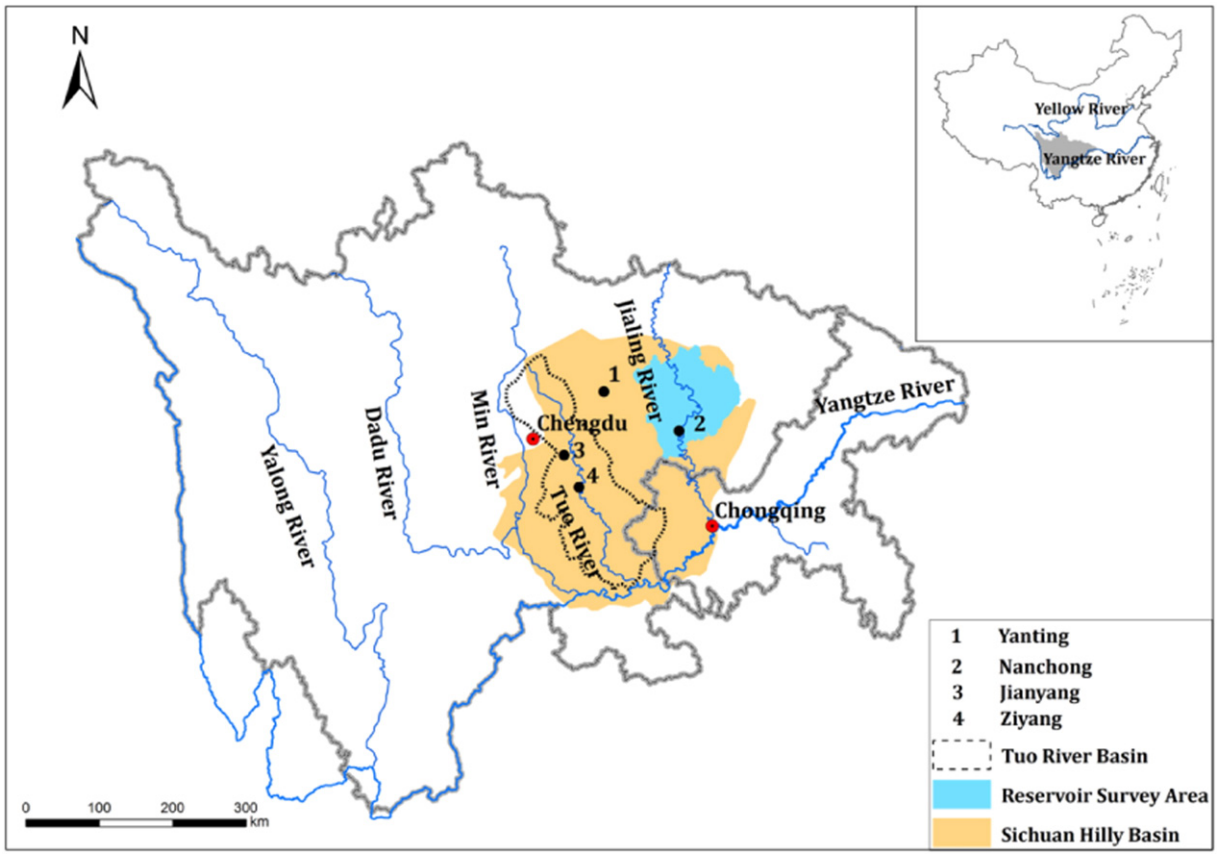

Fig. 1. Map of the Sichuan Hilly Basin in Southwestern China, with the selected study sites and the Tuo River basin shown.

was impounded by an earthen dam (~4.5 m high) during the period from 1949 to 1956, with storage capacity ranging between 1.5 and 5.1×10^4 m^3. The dams were made of soil dug from the valley bottoms within the ponds. The ponds have simple water delivery facilities comprising weirs or bottom culverts with intakes. The storage water in the ponds is used for irrigation in spring and summer. The pond in the Jiliu study catchment has no flood spill ditches, whereas the pond in the Wujia catchment has an overflow ditch that is seldom used. The pond in the Tianmawan catchment has a flood spill ditch that was seldom used until 1981, but after reorganization of the land management system that year, it has since been used to divert floods with high sediment concentrations away from the pond basin. Sediments may pass through the dams via the spillways and may be returned to the land via irrigation. Extensive survey of 79 ponds and reservoirs (see in Fig. 1) were presented to evaluate changes of sediment yields with spatial scales. The Tuo River has a channel length of 712 km, of which a major portion flows through the SHB. Runoff and sediment yield from the Tuo River reflect both local natural and anthropogenic controls on hydrological processes.

2.2. Methods

2.2.1. Approaches

We used data from multiple monitoring approaches to assemble information on sediment production and redistribution at hillslope, first-order small catchment and river basin scales. The monitoring techniques encompassed fallout radionuclide tracing, runoff plot observation, core chronology dating, and conventional sediment flux monitoring. The combination of datasets permitted quantification of sediment yields at multiple spatial (from hillslope field to first-order catchment and drainage basin) and temporal scales (from the recent time to past decades).

2.2.2. Use of fallout radionuclides to estimate soil erosion rates on cultivated land

Radionuclide datasets were used for evaluation of sediment redistribution rates at the field scale. Core samples for local ^{137}Cs reference inventories were collected depending on local landscape conditions and included flat grassland or non-irrigated flat cultivated fields as well as

Table 1
Major characteristics of the four primary study sites selected and principal monitoring approach generating the data used in this study.

Variables	Yanting	Nanchong	Jianyang	Ziyang
Landform	Hilly	Hilly	Hilly	Hilly
Precipitation	826 mm	1010 mm	874 mm	958 mm
Soil	Jurassic Penglaizhen Group	Jurassic Suining Group	Jurassic Suining Group	Jurassic Suining Group
Monitoring approach	CCD	FRT, CCD, SB	RPO	RPO
Study scale	First-order catchment	Hillslope and first-order catchment	Hillslope	Hillslope

CCD – core chronology dating; FRT – fallout radionuclide tracing; RPO – runoff plot observation; SB – sediment budgeting.

old terraces (Zhang et al., 2003, 2006b). Bulk soil core samples were collected at each of the reference sites from 4 to 12 sampling points, using steel tubes with an inner diameter of 70–80 mm up to a constant depth of 30 cm. An additional sample was collected from 2 to 3 sampling points to a depth of 30–60 cm, to assess the possibility of deeper penetration of ^{137}Cs and ^{210}Pb$_{ex}$ into the local soil profiles. The vertical distribution of ^{137}Cs in the soil profile at each reference location was examined by collecting depth-incremental samples at increments of 3–5 cm down to a total depth of 30–40 cm at one of the sampling points at each site. The traditional transect approach was used to assess the redistribution of ^{137}Cs along the sampled cultivated slopes. Between three to six sampling points were selected along each of the slope transects, according to the slope profile complexity. Three to four bulk samples (0–30 cm depth) were collected at each sampling point using the same steel tubes and these were thoroughly mixed into a single sample to account for the micro-spatial variability of the ^{137}Cs and ^{210}Pb$_{ex}$ inventories associated with cultivated surface micro-topography, variable plough layer thickness and initial fallout variability. In addition, some sampling points were located within potential depositional areas along the lower terrace boundaries (both cultivated and grass slopes). Sectioned cores were collected at these locations to evaluate the total ^{137}Cs inventories in the sampled soil profiles.

All samples were weighed, air-dried, re-weighed after drying, disaggregated by grinding, sieved using a 2-mm mesh and homogenized. Representative sub-samples of sufficient mass (~250 g) were then placed into plastic containers of specific geometry (101 mm inner diameter and 25 mm high) and sealed for 28 days to ensure equilibrium between ^{226}Ra and ^{222}Rn. Radioactivity was measured by γ spectrometry with a high-resolution, low-background, low-energy, hyperpure N-type germanium coaxial detector coupled to an amplifier and multichannel analyzer. The ^{137}Cs activity was measured at the 662 keV peak. The counting time was sufficient to determine the ^{137}Cs isotope activity with a maximum relative error of ±6% at the 95% level of confidence. The conversion models used to convert ^{137}Cs concentrations in the soil cores to sediment redistribution rates along the slopes are described elsewhere (Zhang et al., 2003, 2006b).

Despite the fact that the ^{137}Cs technique has been applied globally to provide quantitative soil redistribution estimates (Zapata, 2010; Matisoff and Whiting, 2011), older and more recent work has highlighted potential problems and uncertainties for the underpinning assumptions (Sutherland, 1994, 1996; Parsons and Foster, 2011, 2013; Kirchner, 2013; Zhang, 2014), to which the fallout radionuclide user community provided a response (Mabit et al., 2013). Zhang et al. (2015) noted the lack of systematic sensitivity or uncertainty analyses for evaluating the soil erosion conversion models. In response, Zhang et al. (2015) undertook such analyses for three widely-used conversion models. The results suggested that soil redistribution estimates are extremely sensitive to ^{137}Cs reference and target sample inventories, but less sensitive to factors such as bulk density, tillage depth and the incorporation of a particle size correction factor in the models. Similarly, uncertainty analysis showed that spatial variabilities of ^{137}Cs inventories in both reference and target location sites are the major components of the total uncertainty associated with soil erosion estimates, followed by the particle size correction factor used in the conversion models. Factors such as bulk density and tillage depth were shown to make minor contributions to total uncertainty. Although the work by Zhang et al. (2015) reported that random spatial variations in ^{137}Cs distribution, hamper the use of the technique for estimating point soil redistribution rates, these random variations can be overcome statistically by increasing independent sample numbers and interpreting soil redistribution rates in terms of mean values for uniform landform units or contour transects since the random errors tend to cancel out if averaged over a uniform area.

2.2.3. Use of erosion plots to estimate soil erosion rates on cultivated land

In view of the limitations and uncertainties identified for soil erosion estimation based on ^{137}Cs measurements (see above), the results generated using the fallout radionuclide conversion models were compared with independent evidence based on direct monitoring of soil loss using bounded runoff plots (Yang, 1997; Lin et al., 2009) located in the SHB. All plots are 20 m in length and 5 m in width with a concrete boundary. The use of bounded runoff plots is widely reported in the international literature, but again, some important limitations and uncertainties should be borne in mind when interpreting erosion plot data (Collins and Walling, 2004; Boix-Fayos et al., 2006). The deployment of boundaries introduces so-called 'boundary effects' and thereby reduces the representation of wholly natural conditions (Bagarello and Ferro, 1998; Nearing et al., 1999). As a result, some researchers have deployed unbounded plots (Loughran, 1989). Other issues with bounded plots include exhaustion effects and unrepresentative coverage of micro-environments on slopes (Boix-Fayos et al., 2006). Erosion plot estimates must be based on long-term monitoring and multiple replicates to generate reliable data (Elwell, 1990; Ollesch and Vacca, 2002). Uncertainties are typically associated with the collection of representative water samples at the plot outlets due to either sedimentation in collection tanks or unrepresentative sampling by automated samplers (Morgan, 1995). The results from both the ^{137}Cs tracing and traditional erosion plot observations were combined with information on land use to calculate the slope sediment budget term for the Tianmawan study catchment.

2.2.4. Use of sediment profile dating and bathymetric surveys to measure sediment storage in ponds and estimate suspended sediment yields

Total sediment volume in dams can be directly measured by geometric surveying, and dry sediment mass can be estimated using a density index. Sediment yield from the upstream catchment can thus be quantified applying a trapping efficiency factor (Mekonnen et al., 2015). Assessment of sediment storage in the key study areas was undertaken using the ^{137}Cs technique for sediment profile dating and bathymetric surveys. Depth-incremental sampling was used to permit the determination of ^{137}Cs vertical depth profiles for the different sediment sinks (dry/wet ponds and floodplains). Samples from ponds with water were collected by drilling a single core with a diameter of 98 mm into the pond bed at the centre of each basin. In these cases, a PVC pipe with a diameter of 100 mm was used to protect the core during the drilling and subsequent extraction (Zhang et al., 2006a). The resulting ^{137}Cs vertical depth profiles for each sampled core were used to calculate the sediment volumes deposited within the sediment sinks over the different time intervals revealed by the ^{137}Cs chronologies. A detailed geodetic survey was conducted for each pond or floodplain sampling site using a digital tacheometer to document their detailed longitudinal profiles and total surface areas.

A number of uncertainties need to be borne in mind when interpreting ^{137}Cs chronologies for deposited sediment profiles. Downward diffusion or migration can influence the depth at which ^{137}Cs first appears, but such problems are generally more likely in floodplain than lake or pond profiles, where bioturbation will be more restricted by prevailing environmental conditions. ^{137}Cs is generally considered more mobile than ^{210}Pb and a number of factors can increase the risk of ^{137}Cs remobilization including the presence of ammonium and reduced oxygen levels (Walling and Foster, 2016). Interpretation of ^{137}Cs chronologies in sediment profiles in the context of fallout patterns is most reliable in the absence of any significant change in sediment source over the time period in question that may have drastically changed the ^{137}Cs content of the deposited sediment (cf. Foster and Rowntree, 2012). The limitations of using a single-core approach have been reported in the international literature (Dearing, 1986; Foster, 2006, 2010; Foster et al., 2011) but the use of multiple cores is generally cost prohibitive. Additional uncertainties are associated with obtaining reliable estimates of dry bulk density for estimating the sediment mass in storage and of trap efficiency which can vary over time (Dearing, 1986; Verstraeten and Poesen, 2000).

Information on total sedimentation was collected for 79 ponds and reservoirs within the different study catchments (Fig. 1). The sediment volumes in ponds and reservoirs were determined based on detailed depth measurements taken along representative cross-sections. The number of cross-sections depended on water body size. Total sedimentation was determined based on the differences between the documented initial bottom surface area at the time of pond construction and bottom surface area on the date of the field survey. The majority of reservoirs in the SHB were constructed during the 1950s.

2.2.5. Use of conventional monitoring to estimate suspended sediment yields

The estimation of suspended sediment yields requires data on discharge and sediment concentrations (de Vries and Klavers, 1994). River discharge and suspended sediment load estimates (1957–2000) at the final downstream station on the Tuo River, were collected by the Yangtze River Water Conservancy Committee under the Ministry of Water Resources of China. Hydrological measurements follow national standards to ensure accuracy and consistency. At each station, replicate vertical profiles of the river channel are arrayed, and both depth and flow velocity are measured throughout the cross section. Water discharge is calculated by the cross-section area and mean flow velocity. Suspended sediment concentration is determined by water sampling based on hydrology stage. Suspended sediment load is the product of water discharge and sediment concentration and the load is normalized by the catchment area to generate estimates of annual specific suspended sediment yield.

Estimates of river discharge are typically reliable only within ±20% (Sauer and Meyer, 1992; McMillan et al., 2012; Lloyd et al., 2016). The frequency, number and timing of water samples for the determination of suspended sediment concentrations will impact significantly on the precision, bias and accuracy of the data assembled for concentrations, loads and specific yields (de Vries and Klavers, 1994; Phillips et al., 1999; Moatar and Meybeck, 2005; Horowitz, 2013). Recent work by Horowitz et al. (2015) has indicated that calendar-based and random-based water sampling strategies for suspended sediment should consider scale in that larger sample sizes are required as drainage basin scale decreases and, hydrology-based sampling strategies are likely to generate the most reliable estimates of sediment flux with the fewest samples, regardless of catchment size.

3. Results and discussion

3.1. Soil erosion on upland cultivated fields

For the four sites selected to quantify soil erosion using fallout radionuclide tracing and runoff plot observations, cultivated fields are located on steep concave slopes with gradients ranging from 5 to 35° as dry farmlands and on valley bottoms as paddy fields with gradients close to 0°. There is no erosion on paddy fields except in extreme high flooding with low return intervals. The cultivated fields typically occupy 30–40% of the total area of the first-order catchments. The typical lengths of sloping fields are 5–35 m, parts of which are terraces that mainly occupy the steepest slopes. According to the fallout radionuclide data, erosion from fields with a length of <10 m and a gradient ≤5° is low, with an annual loss of 800 $Mg \cdot km^{-2} \cdot yr^{-1}$ (Table 2). However, estimated soil losses based on the same method increase considerably on steeper slopes (10–20°) with lengths ranging from 7 to 24.7 m, up to a mean annual loss of 4501 $Mg \cdot km^{-2} \cdot yr^{-1}$. The proportion of cultivated slopes with steepness 10–20° is <10% of the total area of cultivated fields based on field observations. In comparison, the corresponding respective estimates for the two slope categories based on traditional bounded plot experiments were 600 $Mg \cdot km^{-2} \cdot yr^{-1}$ and 3300 $Mg \cdot km^{-2} \cdot yr^{-1}$ according to the latest monitoring data (Lin et al., 2009). Collectively, the estimates of soil loss provided by the two techniques appear feasible in the context of current understanding of global erosion rates (García-Ruiz et al., 2015). The simple comparison of estimated soil erosion rates implies that for both slope categories, the estimates of soil erosion by fallout radionuclides are marginally higher (1.33 times higher for 5° and 1.36 times higher for 10–20°) than those generated by runoff plot studies, albeit in recognition of the inherent uncertainties associated with both measurement techniques and the fact that this comparison is not based on consistent study sites nor measurement periods (given that the temporal basis of the radionuclide estimates covers the last ~50 years and the monitoring for the plot studies covers a shorter more recent study period).

3.2. Sediment redistribution within headwater catchments and associated sediment yields

The Tianmawan catchment was selected to understand the slope-valley connectivity in the sediment budgets at catchment scale. There are two groups of terraces in this catchment: gentle terraces with mean slopes of 5° and slope lengths of <10 m and, relatively steep terraces with slopes of 10–20° and slopes lengths of 15–20 m. The soil losses on terraces were determined using both radionuclide tracing and more traditional bounded plot experiments (Table 3). These techniques were shown above to give broadly similar estimates of typical soil loss from hillslopes, especially in the case of the steeper slopes. The total deposited sediment volume (taken to represent SSY) for the period 1963–1981 was determined based on ^{137}Cs chronologies in pond deposits (Fig. 3) and the corresponding pond surface areas. The cored ponds were located at the catchment outlets. Additionally, the possibility for sediment deposition in the paddy fields located upstream from the ponds was assessed. New land created by silting at the upstream delta of the pond has been brought under cultivation as paddy

Table 2
Comparisons of mean annual net soil losses from upland cultivated hillslopes using ^{137}Cs tracing (CS), combined ^{137}Cs and $^{210}Pb_{ex}$ tracing (CSP) and traditional erosion plot monitoring (PM).

Site Location	Mean annual precipitation (mm)	Average slope length (m)	Average slope gradient (°)	Method	Time interval	Average soil erosion rates ($Mg \cdot km^{-2} \cdot yr^{-1}$)	Cultivation method	Reference
Nanchong	1010	9	5	CS	1964–2000	758	Cultivated terrace	(Zhang et al., 2003)
		17	11			4663	Cultivated terrace	(Zhang et al., 2003)
		24.7	14			6780	Cultivated terrace	(Zhang et al., 2003)
Jianyang	874	7	20	CSP	1954–2008	4870	"Tiaoshamiantu"[a]	(Zhang et al., 2006b)
		10	10			1691	"Tiaoshamiantu"[a]	(Zhang et al., 2006b)
Ziyang	950	20	10	PM	1989–1995	2590	Cultivated plot	(Yang, 1997)
		20	15	PM	1989–1995	4221	Cultivated plot	(Yang, 1997)
Ziyang	966	20	20	PM	1998–2005	3250	Cultivated plot	(Lin et al., 2009)
		20	20	PM	1998–2005	220	Cultivated plot with vetiver hedgerows through 6,2 m	(Lin et al., 2009)
		20	20	PM	1998–2005	365	Cultivated plot with indigo hedgerows through 6,2 m	(Lin et al., 2009)

[a] Note eroded sediment settled in ditches was manually returned to the field by farmers.

Table 3
Sediment budget estimates for the Tianmawan catchment.

	Mean annual soil erosion rate ($Mg \cdot km^{-2} \cdot yr^{-1}$)	Area (km^2)	Annual soil loss (1963–2004) (Mg)	Annual sediment storage (Mg) (1963–1981)	Annual sediment delivery ratio
Soil erosion estimated by radionuclide tracing on cultivated terraces with a mean slope of 5°	800	0.07	56		
Soil erosion estimated by radionuclide tracing on cultivated terraces with a mean slope of 10–20°	4501	0.015	67.5		
Annual soil loss			123.5		
Sediment deposition in the pond				107	0.87
Soil erosion estimated by runoff plots on cultivated terraces with a mean slope of 5°	600[a]	0.07	42		
Soil erosion estimated by erosion plots on cultivated terraces with a mean slope of 10–20°	3300[b]	0.015	49.5		
Annual soil loss			91.5		
Sediment deposition in the pond				107	1.17

[a] Based on the relationship between slope gradient and soil loss which has been established using Chinese observations (Liu et al., 1994).
[b] Based on plot study (1998–2005) data (Lin et al., 2009).

fields in the Tianmawan catchment. However, local farmers were unable to distinguish the new paddy fields from the old fields because the pond was constructed so long ago (during the 1950s). This particular study pond was found to have very limited sediment deposition based on the ^{137}Cs depth distribution curve for the paddy field, which is located near the pond.

Based on available data for the Tianmawan catchment, it was possible to estimate the sediment budgets using the different magnitudes of the soil erosion term based on the alternative methods. The different time intervals used as a basis to calculate soil loss and sedimentation rates are an important source of uncertainty in the estimated sediment budgets. Using the radionuclide based estimates for soil erosion, the total soil losses exceed sediment deposition in the pond, yielding a SDR of 0.87 (Table 3). However, it is likely that a proportion of the mobilized sediment overflowed the dam during extreme events, thereby introducing one source of uncertainty in this comparison. It is also important to bear in mind that some extent of error exists in determining the total volume of sediment accumulated in the pond over the time period represented by ^{137}Cs, because it was determined using only one sediment core and there are known problems with characterizing sediment bulk density especially for historical deposits. In contrast, the corresponding SDR estimated using the erosion plot data to calculate the soil erosion term of the sediment budget was 1.17 (Table 3). The contrasting SDRs for the two budgets is a product of the uncertainty associated with both methods for estimating the soil erosion rates for different slope gradients as well as the use of a single-core approach for evaluating sediment storage in the pond.

Contrasting estimates of hillslope soil erosion in the Tianmawan catchment were calculated using the radionuclide ($123.5\ Mg \cdot yr^{-1}$) and runoff plot ($91.5\ Mg \cdot yr^{-1}$) methods (Table 3). This comparison, however, is not based on consistent study slopes or experimental duration. It is feasible to suggest that mean annual soil losses from cultivated terraces was slightly higher in particular during the 1960s–70s, because a clear trend of decreasing total precipitation and rainfall intensity was identified for the SHB from the middle to the end of 20th century. This is likely to be a factor in the magnitude of the rates based on ^{137}Cs in the context of the fallout history of that particular radionuclide (cf. Porto et al., 2013). In contrast, both sets of plot observation data were collected during the 1990s and the beginning of the 2000s and so coincide with the period of lower rainfall totals and intensities. It is also likely that erosion rates determined using both ^{137}Cs and $^{210}Pb_{ex}$ are influenced by losses independent of water, tillage and wind erosion due to the local harvesting of sugar beet and potatoes. According to existing data, soil losses accompanying the harvesting of root crops are as high as 500–600 $Mg \cdot km^{-2} \cdot yr^{-1}$ with large harvesting equipment (Poesen et al., 2001). In the context of the higher estimates of soil loss based on radionuclides (200–1200 $Mg \cdot km^{-2} \cdot yr^{-1}$ higher for the two slope categories) and the size of the harvesting equipment in the study area, it is likely that such losses are partly responsible for the differences in the estimated erosion rates in Table 3, but the ongoing need to test the principal assumptions of radionuclide-based assessments (Parsons and Foster, 2011) and to recognise and attempt to quantify the inherent uncertainties (Zhang et al., 2015) must be borne in mind here. Ongoing work by some researches has been testing the ^{137}Cs approach for the estimation of soil loss in different environments (Mabit et al., 2008, 2013) using long-term sediment yield monitoring data for micro-catchments (Porto et al., 2001, 2003, 2016), erosion models (Hancock et al., 2008) or a combination of different methods and techniques (Golosov et al., 2008) and these studies provide validation of ^{137}Cs-based soil erosion data at micro-scales. In recognition of the uncertainties associated with the ^{137}Cs-based approach, however, and the continued need for detailed systematic evaluation of the assumptions underpinning fallout radionuclide assessments of soil erosion in different types of environment, this study assembled soil erosion rates predicted using both radionuclide methods and unit erosion plots in recognition of the need to interpret the former carefully in the context of alternative independent data for this particular component of the catchment sediment budget. In the case of this study, and again bearing in mind the inherent sampling and measurement uncertainties associated with the different approaches and additional potential contributing factors discussed above, the impact of the slightly higher erosion rates predicted using ^{137}Cs is accentuated by scaling up to estimate the SDR of the sediment budget (Table 3). Using either estimate of the soil erosion term suggests, however, that zero-order catchments are characterized by very high SDRs. High SDRs are normally associated with corresponding high sediment system sensitivity to environmental and anthropogenic controls (Walling, 1999).

The SSY was also determined using ^{137}Cs chronologies for the two other study catchments (Wujia and Jiliu). These ^{137}Cs-based SSYs for deposition in the ponds were estimated from the deposition volumes on the basis of the dateable ^{137}Cs peak horizons, the elapsed time since pond construction, trap efficiency, sediment bulk density ($1.4\ Mg \cdot m^{-3}$) and upstream catchment areas. No corrections were made for autochthonous sediment inputs associated with organic matter production, shoreline inputs (most severe immediately after post construction) or atmospheric inputs (cf. Foster, 2010).

In 1956, a small reservoir was constructed at the outlet of the Wujia catchment for irrigation purposes. The Wujia catchment is very small and characterized by steep terrain. The eroding purple soil is very fine (99% of the particles are <0.5 mm in diameter). Field investigations indicated that no significant deposition occurred in the gully bottom upstream from the reservoir. The reservoir has a current storage capacity of 25,000 m^3 with a maximum water depth of 3.0 m and a surface area of 9200 m^2. This dam has a spillway and bottom culvert with several intakes on the left side. The maximum sediment deposition depth since 1956 was 1.3 m and 5000 m^3 of sediment had been deposited in

the reservoir, which was estimated from the changes in its water storage volume. Parts of the fringe areas in the reservoir were dredged in 1985 and this should be borne in mind. Based on the deposited sediment volume in the reservoir (since 1956), the SSY of the Wujia catchment was estimated to be 701 $Mg \cdot km^{-2} \cdot yr^{-1}$. In the Jiliu study catchment, a grey green fine sand layer was found in the deposited sediment profile (Fig. 2). It is most likely to be associated with sediment delivered to the pond in 1984, when a road was constructed in this catchment. The estimated annual average SSY for the period 1984–2003 was 584 $Mg \cdot km^{-2} \cdot yr^{-1}$, which is less than that during the period 1963–1983.

3.3. Wider evidence on suspended sediment yields at multiple catchment scales

The estimated SSYs for 79 additional catchments, calculated from a more strategic reservoir sediment survey, varied between the groups (Table 4). However, the estimated SSYs increased from small ponds

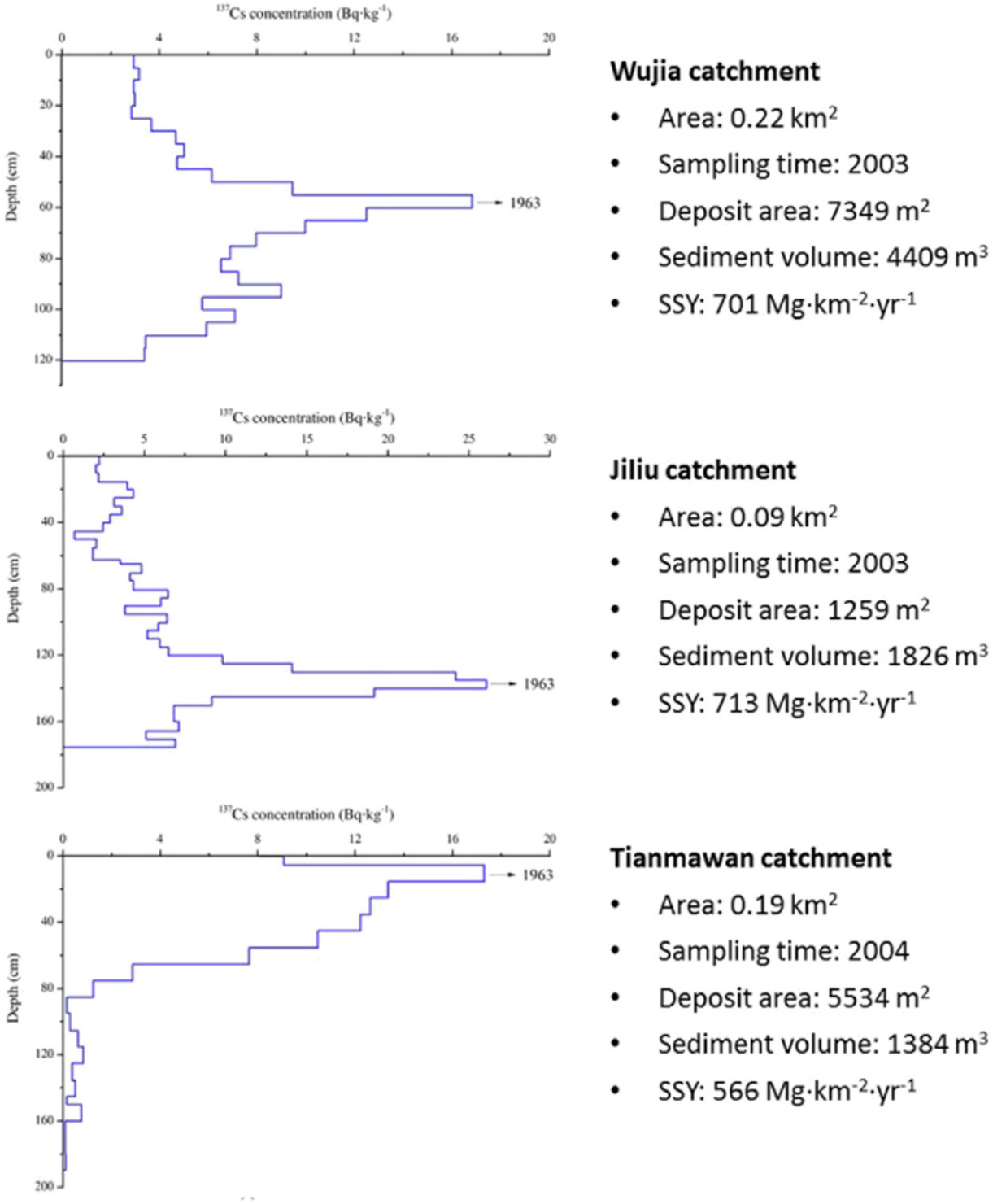

Fig. 2. ^{137}Cs depth distribution along sediment cores extracted from ponds at (a) Wujia catchment (upper plot), (b) Jiliu catchment (middle plot), (c) Tianmawan catchment (lower plot).

Table 4
Specific sediment yields (SSY) calculated from pond and reservoir deposits.

Sediment sink	Catchment area (km^2)	Number of ponds	Mean catchment area (km^2)	Specific sediment yield (Mg km^{-2} yr^{-1})				
				Mean	Max	Min	Standard deviation	CV (%)
Small field ponds	<0.25	60	0.11	641	1568	79	686	60
Large field ponds	0.25–2	4	1.02	762	958	632	142	19
Small reservoir	2–15	9	9.6	849	2238	71	676	80
Medium reservoir	15–60	6	39.3	733	1780	306	474	65

(79–1568 $Mg \cdot km^{-2} \cdot yr^{-1}$), large ponds (632–958 $Mg \cdot km^{-2} \cdot yr^{-1}$) to small reservoirs (71–2238 $Mg \cdot km^{-2} \cdot yr^{-1}$) with a subsequent reduction when scaling up to medium reservoirs (306–1780 $Mg \cdot km^{-2} \cdot yr^{-1}$). The estimated mean SSYs for the different pond/reservoir groups are 641 (N = 60), 762 (N = 4), 849 (N = 9) and 733 (N = 6) $Mg \cdot km^{-2} \cdot yr^{-1}$, respectively. The range of estimated SSY in each pond/reservoir group was broadly similar, although much less in the case of large field ponds. There is some increase in SSYs from small ponds to small reservoirs with catchment areas of <15 km^2. Gully and bank erosion may be responsible for some of this increase in estimated SSYs, particularly given the relatively high channel gradients and high intensity of weathering (up to 1.2 $cm \cdot yr^{-1}$). However, direct comparisons between the estimates should bear in mind uncertainty arising from different land use proportions in the different catchments. More detailed study should be undertaken to help improve the interpretation of these SSY estimates on the basis of key catchment characteristics.

The high variability in SSY estimates for each group of ponds and reservoirs has two likely principal causes. The first is the high variability of soil erodibility due to differences in parent rocks. For example, even heavy rain-storms with a mean rainfall intensity of around 80 mm per hour produce very low runoff (runoff coefficient < 0.01) in zero-order catchments with permeable sandstone parent rocks and sandy loam soil (Yang et al., 2009). The second cause is the spatial and temporal variability of land use over the last 50–60 years within the individual catchments. The proportion of arable land, forest and wasteland has not remained uniform. Additionally, individual cultivated fields may have different crop rotations over time and thereby varying risks of soil erosion and sediment loss. All of these factors can potentially influence the variability of estimated SSYs for individual small catchments over time.

3.4. Preliminary data interpretation in the context of potential climatic and anthropogenic drivers

It is typical in the SHB for SSY to increase with catchment area up to 10 km^2, due to the increased contribution of gully/bank erosion with increasing scale (Fig. 3). The relative contribution of erosion under the forest (not included in the soil loss data reported herein) and in the gullys of the SHB, according to results from the application of the source fingerprinting technique, can reach 40–45% of total sediment production. However, it would be constructive to measure gully wall and river bank retreat directly for its accurate quantitative assessment in terms of gross contribution to the catchment sediment budget. Sediment budget terms are also required to represent sediment losses from wastelands under the forest and without canopy cover as a means of providing a more comprehensive understanding of the local natural processes releasing sediment.

The rates of bank erosion decrease, with increasing basin area, due to the increasing proportion of flat paddy fields (valley bottoms) that are not producing additional net sediment loss to the channel. Thus, it is possible to expect some decrease in SSY with a basin area increase in river catchments with an area of <100 km^2, even in the case of the typically extremely low floodplain sedimentation rates in the SHB. This interpretation should be confirmed by direct measurements on floodplains, but the intensive use of all floodplains as cultivated land (mostly paddy land) and the deep incision of local river channels into parent rocks provide partial confirmation of this interpretation. However, if we compare the mean annual SSY of the Tuo River (basin area 23,283 km^2; Fig. 1) from 1957 to 1966 (Fig. 4) with the mean annual SSY for medium size reservoirs (<60 km^2) from 1950 to 2000, we do not find any differences. Thus, it is more likely that soil losses from zero-order catchments were higher in the 1957–1966 period. This is also confirmed by the ^{137}Cs depth distribution profiles in the cored ponds, where ^{137}Cs was found to be 40–60 cm deeper than the ^{137}Cs peak. Initial ^{137}Cs fallout occurred in 1954, so it is likely that soil loss was highest between 1957 and 1966. A sharp increase in the number of ponds and particularly, water storage reservoirs during the late 1950s–1960s led to a considerable decrease in both water discharge and sediment yield during the period 1967–1984, compared with previous time intervals. However, it is more likely that soil losses from cultivated fields did not decrease considerably in that time period as soil erosion conservation was not being implemented during this period. Soil erosion has been accelerated significantly by intensive land use practices during the period 1950s–1980s. Unused land was extensively reclaimed to meet increasing food demand due to population growth during the 1950s–1970s. The establishment of the Household Responsibility System in the early 1980s greatly motivated local farmers to make

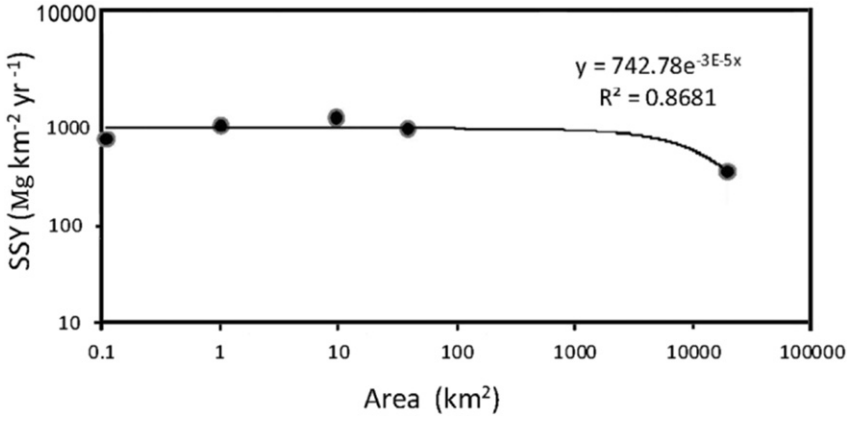

Fig. 3. The relationship between specific sediment yield (SSY) and catchment area for small catchments in the Sichuan Hilly Basin.

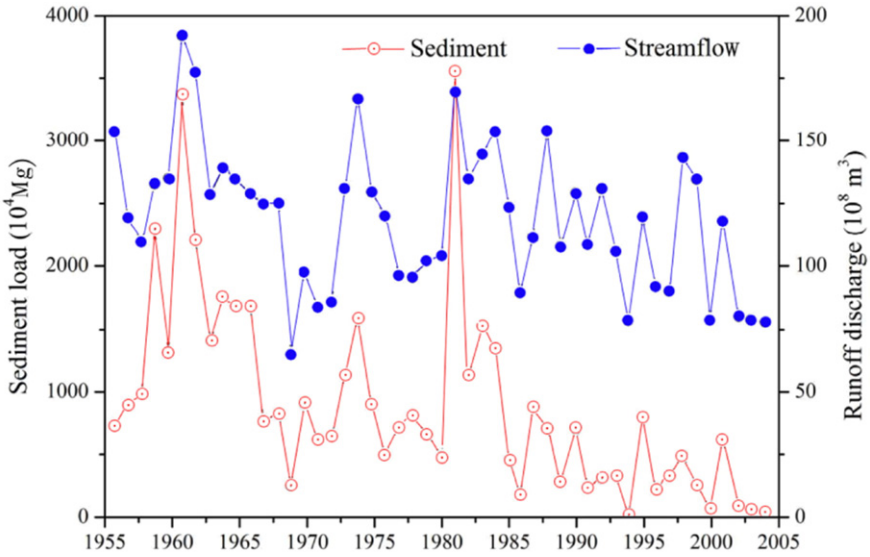

Fig. 4. Temporal changes in annual average runoff discharge and suspended sediment load for the Tuo River basin.

full use of their land. This is also partially confirmed by the sharp increase in SSY in 1982 (Fig. 4), which was more likely associated with a few extreme rainfall events. By realizing that severe soil erosion threatens sustainable land use and causes significant downstream flooding and sedimentation, multiple conservation schemes have been implemented in this region since the 1980s. Engineering measures (terracing) have been introduced to protect fertile topsoil loss under arable land use. The "Grain for Green Programme", launched in 1999, aims to transfer cultivated hillslopes with gradients greater than 25° to forest or grassland. Land use changes have taken place in conjunction with reforestation and urbanization. It is more likely that the gradual increase in area under the forest in the SHB and crop rotation changes since the mid 1980s considerably influenced the decreasing SSY during the period 1985–2000, compared with 1967–1984 (Fig. 4). Simultaneously, there was a clear decreasing trend in maximum rainfall intensity during the summer months in the SHB since 1990. There has also been some decrease in summer precipitation (Huang et al., 2014). Thus, both natural factors and soil conservation measures are likely to be responsible for the decreasing SSYs measured during the period 1985–2000 (Fig. 4 and Table 5).

The SHB is characterized by very high slope-channel connectivity and this results in efficient transport of the majority of eroded sediment from zero-order catchments to main river channels. In terms of the estimated SSYs from the zero-order catchments in the SHB, the estimates provided by this study are broadly comparable to those observed around the world (Walling, 1983), particularly given the relatively high proportion of naturally-induced erosion (gully and wastelands). However, the subsequent sediment transfer along the fluvial drainage system into higher order river channels is completely different. In the SHB, even for river basins with an area of >20,000 km^2, the SSY exceeds 400 Mg·km^{-2}·yr^{-1} (Lu and Higgitt, 1999). This can be explained by the very low sedimentation along the pathways from the slope catchments to the main river valleys and on the river floodplains which results in high SDRs regardless of increasing catchment scales.

Table 5
Temporal variations in runoff discharge and specific suspended sediment yield (SSY) in the Tuo River basin.

Period	Mean annual runoff discharge (10^8 m^3)	Mean annual SSY (Mg·km^{-2}·yr^{-1})
1957–1966	140	759
1967–1984	119	441
1985–2000	113	177
1957–2000	122	417

4. Conclusions

Soil erosion and sediment production at hillslope field, first-order small catchment (<0.25 km^2) and drainage basin scales in the Sichuan Hilly Basin generated by multiple approaches were synthesized and interpreted in the context of potential climatic and human controls. Mean annual soil erosion rates ranged from 800 Mg·km^{-2}·yr^{-1} to 4500 Mg·km^{-2}·yr^{-1} on the basis of fallout radionuclide tracing and from 600 Mg·km^{-2}·yr^{-1} to 3300 Mg·km^{-2}·yr^{-1} using runoff plot monitoring on selected cultivated hillslopes. Slope-channel connectivity is high, meaning that the majority of eroded sediment from upland cultivated hillslopes is transported directly to the main river channels. A clear decreasing trend in soil erosion rates (400–500 Mg·km^{-2}·yr^{-1}) has been observed over the last 20–25 years and a consistent pattern has, in turn, been observed in monitored SSY. Declining rainfall totals and intensities are likely to be a factor controlling these consistent trends in soil erosion and SSY. The implementation of soil conservation practices is also likely to have contributed to the reduced soil losses and sediment transfers to, and through, the fluvial system. Given the high SDRs estimated using the sediment budgeting approach discussed herein, fluvial SSY serves as a direct indicator of soil loss. Therefore, it may be possible to forecast the reduction of sedimentation rates in the Three Gorges Reservoir (TGR) on the basis of these trends of decreasing soil losses and SSY from the SHB, since sediment input from upstream catchments contributes ~86.7% of total sediment discharge to the TGR.

Acknowledgements

This work was supported by the Key Laboratory of Mountain Surface Processes and Ecological Regulation, Chinese Academy of Sciences, and the Russian Foundation for Basic Research and National Natural Science Foundation of China (Grant 14-05-91153). Rothamsted Research receives strategic funding from the UK Biotechnology and Biological Sciences Research Council (BBSRC). The input from ALC to this work was funded by a Chinese Academy of Sciences (CAS) Visiting Professorship. QT is supported by a Royal Society Newton International Fellowship and is hosted by Rothamsted Research under the supervision of ALC.

References

Bagarello, V., Ferro, V., 1998. Calibrating storage tanks for soil erosion measurement from plots. Earth Surf. Process. Landf. 23, 1151–1170.

Belyaev, V.R., Golosov, V.N., Kuznetsova, J.S., Markelov, M.V., 2009. Quantitative assessment of effectiveness of soil conservation measures using a combination of Cs-137 radioactive tracer and conventional techniques. Catena 79 (3), 214–227.

Boix-Fayos, C., Martinez-Mena Garcia, M.D., Arnau, R.E., Calvo-Cases, A., Castillo, S.V.M., Albaladejo, M.J., 2006. Measuring soil erosion by field plots: understanding the sources of variation. Earth-Sci. Rev. 78, 267–285.

Chaplot, V., Poesen, J., 2012. Sediment, soil organic carbon and runoff delivery at various spatial scales. Catena 88, 46–56.

Collins, A.L., Walling, D.E., 2004. Documenting catchment suspended sediment sources: problems, approaches and prospects. Prog. Phys. Geogr. 28, 159–196.

Dearing, J.A., 1986. Core correlation and total sediment influx. In: Berglund, B. (Ed.), Handbook of Holocene Palaeoecology and Palaeohydrology. John Wiley & Sons, Chichester, pp. 247–270.

Elwell, H.A., 1990. The development, calibration and field testing of a soil loss and runoff model derived from a small-scale physical simulation of the erosion environment on arable land in Zimbabwe. J. Soil Sci. 41, 239–253.

Evans, J.K., Gottgens, J.F., Gill, W.M., Mackey, S.D., 2000. Sediment yields controlled by intrabasinal storage and sediment conveyance over the interval 1842–1994: Chagrin River, Northeast Ohio, U.S.A. J. Soil Water Conserv. 55, 264–270.

Ferro, V., Minacapilli, M., 1995. Sediment delivery processes at basin scale. Hydrol. Sci. J. 40 (6), 703–717.

Foster, I.D.L., 2006. Lakes in the sediment delivery system. In: Owens, P.N., Collins, A.J. (Eds.), Soil Erosion and Sediment Redistribution in River Catchments. CAB International, Wallingford, pp. 128–142.

Foster, I.D.L., 2010. Lakes and reservoirs in the sediment cascade. In: Burt, T.P., Allison, R.J. (Eds.), Sediment Cascades: an Integrated Approach. John Wiley & Sons, Chichester, pp. 345–376.

Foster, I.D.L., Rowntree, K.M., 2012. Historic land management, rainfall and sediment yield changes in the semi-arid Karoo: a palaeoenvironmental reconstruction and interpretation of sediments accumulating in Cranemere Reservoir, Eastern Cape, South Africa. Z. Geomorphol. Suppl. 56 (Suppl. 3), 131–146.

Foster, I.D.L., Collins, A.L., Naden, P.S., Sear, D.A., Jones, J.I., Zhang, Y.S., 2011. The potential for paleolimnology to determine historic sediment delivery to rivers. J. Paleolimnol. 45 (2), 287–306.

García-Ruiz, J.M., Beguería, S., Nadal-Romero, E., González-Hidalgo, J.C., Lana-Renault, N., Sanjuán, Y., 2015. A meta-analysis of soil erosion rates across the world. Geomorphology 239, 160–173.

Gaspar, L., Navas, A., Machín, J., Walling, D.E., 2013. Using $^{210}Pb_{ex}$ measurements to quantify soil redistribution along two complex toposequences in Mediterranean agroecosystems, northern Spain. Soil Tillage Res. 130, 81–90.

Golosov, V.N., Belyaev, V.R., Kuznetsova, Yu S., Markelov, M.V., Shamshurina, E.N., 2008. Response of a small arable catchment sediment budget to introduction of soil conservation measures. Sediment Dynamics in Changing Environments. vol. 325. IAHS Publ., pp. 106–113.

Golosov, V.N., Belyaev, V.R., Markelov, M.V., 2013. Application of Chernobyl-derived ^{137}Cs fallout for sediment redistribution studies: lessons from European Russia. Hydrol. Process. 27 (6), 781–794.

Hancock, G.R., Loughran, R.J., Evans, K.G., Balog, R.M., 2008. Estimation of soil erosion using field and modelling approaches in an undisturbed Arnhem Land catchment. Geogr. Res. 46, 333–349.

He, X.B., Xu, Y.B., Zhang, X.B., 2007. Traditional farming system for soil conservation on slope farmland in southwestern China. Soil Tillage Res. 94 (1), 193–200.

Hobo, N., Makaske, B., Middelkoop, H., Wallinga, J., 2010. Reconstruction of floodplain sedimentation rates: a combination of methods to optimize estimates. Earth Surf. Process. Landf. 35 (13), 1499–1515.

Horowitz, A.J., 2013. A review of selected inorganic water quality monitoring practices: are we really measuring what we think, and if so, are we doing it right? Environ. Sci. Technol. 47, 2472–2486.

Horowitz, A.J., Clarke, R.T., Merten, G.H., 2015. The effects of sample scheduling and sample numbers on estimates of the annual fluxes of suspended sediment in fluvial systems. Hydrol. Process. 29, 531–543.

Huang, J., Sun, S.L., Xue, Y., Li, J.J., Zhang, J.C., 2014. Spatial and temporal variability of precipitation and dryness/wetness during 1961–2008 in Sichuan Province, West China. Water Resour. Manag. 28, 1655–1670.

Hughes, A.O., Croke, J.C., Pietsch, T.J., Olley, J.M., 2010. Changes in the rates of floodplain and in-channel bench accretion in response to catchment disturbance, central Queensland, Australia. Geomorphology 114 (3), 338–347.

Kirchner, G., 2013. Establishing reference inventories of ^{137}Cs for soil erosion studies: methodological aspects. Geoderma 211–212, 107–115.

Lin, C.W., Tu, S.H., Huang, J.J., Chen, Y.B., 2009. The effect of plant hedgerows on the spatial distribution of soil erosion and soil fertility on sloping farmland in the purple-soil area of China. Soil Tillage Res. 105 (2), 307–312.

Liu, B.Y., Nearing, M.A., Risse, L.M., 1994. Slope gradient effects on soil loss for steep slopes. Trans. Am. Soc. Agric. Eng. 37 (6), 1835–1840.

Lloyd, C.E.M., Freer, J.E., Johnes, P.J., Coxon, G., Collins, A.L., 2016. Discharge and nutrient uncertainty: implications for nutrient flux estimation in small streams. Hydrol. Process. 30, 135–152.

Loughran, R.J., 1989. The measurement of soil erosion. Prog. Phys. Geogr. 13, 216–233.

Lu, X.X., Higgitt, D.L., 1999. Sediment yield variability in the Upper Yantze, China. Earth Surf. Process. Landf. 24, 1077–1093.

Lu, X.X., Ashmore, P., Wang, J., 2003. Sediment yield mapping in a large river basin: the Upper Yangtze River. Environ. Model. Softw. 18, 339–353.

Mabit, L., Benmansour, M., Walling, D.E., 2008. Comparative advantages and limitations of the fallout radionuclides ^{137}Cs, $^{210}Pb_{ex}$ and ^{7}Be for assessing soil erosion and sedimentation. J. Environ. Radioact. 99, 1799–1807.

Mabit, L., Meusburger, K., Fulajtar, E., Alewell, C., 2013. The usefulness of ^{137}Cs as a tracer for soil erosion assessment: a critical reply to Parsons and Foster (2011). Earth Sci. Rev. 127, 300–307.

Matisoff, G., Whiting, P.J., 2011. Measuring soil erosion rates using natural (^{7}Be, ^{210}Pb) and anthropogenic (^{137}Cs, ^{239}Pu, ^{240}Pu). In: Baskaran, M. (Ed.), Handbook of Environmental Isotope Geochemistry. Adv. in Isotope Geochem. vol. 1. Springer-Verlag, Berlin, pp. 487–519.

McMillan, H., Krueger, T., Freer, J., 2012. Benchmarking observational uncertainties for hydrology: rainfall, river discharge and water quality. Hydrol. Process. 26, 4078–4111.

Mekonnen, M., Keesstra, S.D., Baartman, J.E., Ritsema, C.J., Melesse, A.M., 2015. Evaluating sediment storage dams: structural off-site sediment trapping measures in Northwest Etiopia. Cuad. Investig. Geogr. 41 (1), 7–22.

Moatar, F., Meybeck, M., 2005. Compared performances of different algorithms for estimating annual nutrient load discharged by the eutrophic River Loire. Hydrol. Process. 19, 429–444.

Morgan, R.P.C., 1995. Soil erosion and conservation. second ed. Longman, Harlow.

Nearing, N.A., Govers, G., Darrell Norton, L., 1999. Variability in soil erosion data from replicated plots. Soil Sci. Soc. Am. J. 63, 1829–1835.

Ollesch, G., Vacca, A., 2002. Influence of time on measurement results of erosion plot studies. Soil Tillage Res. 67, 23–39.

Owens, P.N., 2005. Conceptual models and budgets for sediment management at the river basin scale. J. Soils Sediments 5, 201–212.

Owens, P.N., Walling, D.E., He, Q.P., Shanahan, J., Foster, I.D.L., 1997. The use of caesium-137 measurements to establish a sediment budget for the Start catchment, Devon, UK. Hydrol. Sci. J. 42 (3), 405–423.

Owens, P.N., Walling, D.E., Leeks, G.J.L., 1999. Deposition and storage of fine-grained sediment within the main channel system of the River Tweed, Scotland. Earth Surf. Process. Landf. 24 (12), 1061–1076.

Oygarden, L., 2003. Rill and gully development during an extreme winter runoff event in Norway. Catena 50 (2–4), 217–242.

Parsons, A.J., Foster, I.D.L., 2011. What we learn about soil erosion from the use of ^{137}Cs? Earth-Sci. Rev. 108 (1–2), 101–113.

Parsons, A.J., Foster, I.D.L., 2013. The assumptions of science. A reply to Mabit et al. (2013). Earth-Sci. Rev. 127, 308–310.

Phillips, J.M., Webb, B.W., Walling, D.E., Leeks, G.J.L., 1999. Estimating the suspended sediment loads of rivers in the LOIS study area using infrequent samples. Hydrol. Process. 13, 1035–1050.

Poesen, J.W.A., Verstraeten, G., Soenens, R., Seynaeve, L., 2001. Soil losses due to harvesting of chicory roots and sugar beet: an underrated geomorphic process? Catena 43 (1), 35–47.

Porto, P., Walling, D.E., Ferro, V., 2001. Validating the use of caesium-137 measurements to estimate soil erosion rates in a small drainage basin in Calabria, Southern Italy. J. Hydrol. 248, 93–108.

Porto, P., Walling, D.E., Ferro, V., Di Stefano, C., 2003. Validating erosion rate estimates provided by caesium-137 measurements for two small forested catchments in Calabria, southern Italy. Land Degrad. Dev. 14 (4), 389–408.

Porto, P., Walling, D.E., Callegari, G., 2011. Using ^{137}Cs measurements to establish catchment sediment budgets and explore scale effects. Hydrol. Process. 25 (6), 886–900.

Porto, P., Walling, D.E., Callegari, G., 2013. Using ^{137}Cs and $^{210}Pb_{ex}$ measurements to investigate the sediment budget of a small forested catchment in southern Italy. Hydrol. Process. 27, 795–806.

Porto, P., Walling, D.E., Capra, A., 2014. Using ^{137}Cs and $^{210}Pb_{ex}$ measurements and conventional surveys to investigate the relative contributions of interrill/rill and gully erosion to soil loss from a small cultivated catchment in Sicily. Soil Tillage Res. 135, 18–36.

Porto, P., Walling, D.E., La Sparda, C., Callegari, G., 2016. Validating the use of ^{137}Cs measurements to derive the slope component of the sediment budget of a small rangeland catchment in southern Italy. Land Degrad. Dev. 27, 798–810.

Ritchie, J.C., Finney, V.L., Oster, K.J., Ritchie, C.A., 2004. Sediment deposition in the flood plain of Stemple Creek Watershed, northern California. Geomorphology 61 (3–4), 347–360.

Sauer, V., Meyer, R., 1992. Determination of error in individual discharge measurements. Open-File Report 92–144. Reston, VA, U.S. Geological Survey.

Sutherland, R.A., 1994. Spatial variability of ^{137}Cs and the influence of sampling on estimates of sediment redistribution. Catena 21, 57–71.

Sutherland, R.A., 1996. Caesium-137 soil sampling and inventory variability in reference samples: literature survey. Hydrol. Process. 10, 34–54.

Trimble, S.W., 2009. Fluvial processes, morphology and sediment budgets in the Coon Creek Basin, WI, USA, 1975–1993. Geomorphology 108 (1–2), 8–23.

Van Oost, K., Govers, G., Desmet, P., 2000. Evaluating the effects of changes in landscape structure on soil erosion by water and tillage. Landsc. Ecol. 15, 579–591.

Verstraeten, G., Poesen, J., 2000. Estimating trap efficiency of small reservoirs and ponds: methods and implications for the assessment of sediment yield. Prog. Phys. Geogr. 24, 219–251.

de Vries, A., Klavers, H.C., 1994. Riverine fluxes of pollutants: monitoring strategy first, calculation methods second. Eur. Water Pollut. Control 4, 12–17.

Wallbrink, P.J., Murray, A.S., 1996. Determining soil loss using the inventory ratio of excess lead-210 to cesium-137. Soil Sci. Soc. Am. J. 60, 1201–1208.

Walling, D.E., 1983. The sediment delivery problem. J. Hydrol. 65 (1–3), 209–237.

Walling, D.E., 1999. Linking land use, erosion and sediment yields in river basins. Hydrobiologia 410, 223–240.

Walling, D.E., 2006. Human impact on land-ocean sediment transfer by the world's rivers. Geomorphology 79 (3–4), 192–216.

Walling, D.E., Collins, A.L., 2008. The catchment sediment budget as a management tool. Environ. Sci. Pol. 11 (2), 136–143.
Walling, D.E., Fang, D., 2003. Recent trends in the suspended sediment loads of the world's rivers. Glob. Planet. Chang. 39 (1–2), 111–126.
Walling, D.E., Foster, I.D.L., 2016. Using environmental radionuclides, mineral magnetism and sediment geochemistry for tracing and dating fluvial fine sediments. In: Kondolf, M., Herve, P. (Eds.), Tools in Fluvial Geomorphology. John Wiley & Sons, pp. 183–209.
Walling, D.E., He, Q., 1997. Use of fallout Cs-137 in investigations of overbank sediment deposition on river floodplains. Catena 29 (3–4), 263–282.
Walling, D.E., He, Q., 1999. Using fallout lead-210 measurements to estimate soil erosion on cultivated land. Soil Sci. Soc. Am. J. 63, 1404–1412.
Walling, D.E., Russell, M.A., Hodgkinson, R.A., Zhang, Y., 2002. Establishing sediment budgets for two small lowland agricultural catchments in the UK. Catena 47 (4), 323–353.
Walling, D.E., Collins, A.L., Jones, P.A., Leeks, G.J.L., Old, G., 2006. Establishing fine-grained sediment budgets for the Pang and Lambourn LOCAR catchments, UK. J. Hydrol. 330 (1–2), 126–141.
Wang, Z., Govers, G., Steegen, A., Clymans, W., Van den Putte, A., Langhans, C., Merckx, R., Van Oost, K., 2010. Catchment-scale carbon redistribution and delivery by water erosion in an intensively cultivated area. Geomorphology 124, 65–74.
Yang, W., 1997. Characteristics and control of soil erosion in a small watershed in the Sichuan Basin. J. Soil Water Conserv. 25 (5), 76–84 (in Chinese).
Yang, J.L., Zhang, G.L., Shi, X.Z., Wang, H.J., Cao, Z.H., Ritsema, C.J., 2009. Dynamic changes of nitrogen and phosphorus losses in ephemeral runoff processes by typical storm events in Sichuan Basin, Southwest China. Soil Tillage Res. 105 (2), 292–299.
Zapata, F., 2010. Handbook for the assessment of soil erosion and sedimentation using environmental radionuclides. Kluwer Academic Publishers, p. 219.
Zhang, X.C., 2014. New insights on using fallout radionulides estimate soil redistribution rates. Soil Sci. Soc. Am. J. 79, 1–8.
Zhang, X.B., Zhang, Y.Q., Wen, A.B., Feng, M.Y., 2003. Assessment of soil losses on cultivated land by using the ^{137}Cs technique in the Upper Yangtze River Basin of China. Soil Tillage Res. 69 (1), 99–106.
Zhang, X.B., Qi, Y.Q., He, X.B., Wen, A.B., Fu, J.X., 2006a. Dating of Reservoir and Pond Deposits by the ^{137}Cs Technique to Assess Sediment Production in Small Catchments of the Hilly Sichuan Basin and the Three Gorges Region, China. IAHS-AISH Publication, pp. 348–354.
Zhang, X.B., Qi, Y.Q., Walling, D.E., He, X.B., Wen, A.B., Fu, J.X., 2006b. A preliminary assessment of the potential for using $^{210}Pb_{ex}$ measurement to estimate soil redistribution rates on cultivated slopes in the Sichuan Hilly Basin of China. Catena 68 (1), 1–9.
Zhang, Q., Xu, C.Y., Zhang, Z.X., Chen, Y.Q., Liu, C.L., 2008. Spatial and temporal variability of extreme precipitation during 1960–2005 in the Yangtze River basin and possible association with large scale circulation. J. Hydrol. 353, 215–227.
Zhang, X.C., Zhang, G.H., Wei, X., 2015. How to make ^{137}Cs erosion estimates more useful: an uncertainty perspective. Geoderma 239–240, 186–194.